Coarse-Grained Molecular Dynamics Study of Permeability Enhancement in DPPC Bilayers by Incorporation of Lysolipid

Nicolas D. Winter and George C. Schatz*

Department of Chemistry, Northwestern University, Evanston, Illinois 60208-3113

Received: November 28, 2009; Revised Manuscript Received: March 9, 2010

The enhanced permeability of flat lipid bilayer membranes at their gel to liquid-crystalline (LC) phase transition has been explored using coarse-grained molecular dynamics. The phase transition temperature, T_m, is deduced by monitoring the area per lipid, the lipid lateral diffusion constant, and the lipid−lipid radial distribution function. We find that a peak in the permeability coincides with the phase transition from the gel to LC state when lysolipid is present. This peak in permeability correlates with a jump in the area per lipid near the same temperature as well as increased fluctuations in the lipid bilayer free volume. At temperatures above T_m, the permeability is only slightly dependent on the amount of lysolipid present. The increased free volume due to the "missing tail" of the lysolipid is partially compensated for by a decrease in area per lipid as the amount of lysolipid increases. We also found that in the coarse-grained model a small amount ($\leq$15 mol %) of lysolipid stabilizes the gel phase and increases the phase transition temperature, while a larger amount of lysolipid (20 mol %) reduces T_m back to that for pure DPPC, and bilayers consisting of $\geq$30 mol % lysolipid did not form a gel phase but still exhibited a peak in permeability near T_m for pure DPPC.

I. Introduction

Drug delivery and release depend greatly on the ability to control the permeability of the vesicle encapsulating the drug. Ideally the drug is safely entrapped inside a vesicle, such as a liposome, until it reaches the target site at which time the drug undergoes triggered release by hyperthermia or a change in pH. Yatvin and Weinstein[1] were among the first to report experiments aimed at triggered release of drugs from liposomes by hyperthermia. It is well-known that the permeability through lipid bilayers exhibits an anomalous peak as the bilayer undergoes the gel to liquid-crystalline (LC) phase transition.[2] The common lipid dipalmitoylphosphatidylcholine (DPPC) undergoes this gel to LC phase transition between 314.65−315.05 K, just above body temperature (310 K).[3,4] This property has caused DPPC vesicles to be recognized as a potential drug delivery agent in conjuction with hyperthermia. The gel phase and LC phase have a number of key differences such as (i) the area per lipid is decreased; (ii) the lipid tails are almost fully extended; and (iii) the lipid lateral mobility is greatly reduced in the gel phase.[5,6] At the phase transition temperature T_m, the gel and LC phases coexist, creating "leaky" interfacial regions due to mismatches in molecular packing and hydrophobic matching.[7] As the lipid membrane is cooled, solid lipid begins to nucleate within the LC phase and as the transformation is completed, grain boundaries are created between the solidifying domains with the grains being oriented at different angles. As the gel membrane is heated, melting initiates at the grain boundaries, forming interfaces between LC and gel phases. It is these "soft" interfaces that are thought lead to the enhanced permeability of the membrane near the phase transition temperature.

The permeability at the phase transition can be enhanced by inclusion of a second lipid component. For example, multilamellar liposomes comprised of dimyristoylPC (diC14) and 10 mol % dicaprylPC (diC10) have been studied experimentally by Risbo et al.[8] The liposomes containing the short chain diC10 lipid were observed to have higher permeability to dithionite ion than pure diC14 vesicles. Risbo describes the increased permeability by a bilayer heterogeneity model in which the shorter chain lipids partition at the grain boundaries and further disturb molecular packing. In a second example, Mills and Needham have shown there is a significant increase in the amount and rate of drug release upon addition of the lysolipid monopalmitoylphosphatidylcholine (MPPC) to DPPC lipid mixtures.[9] Thin layer chromatograpy (TLC) and NMR experiments show that very little lysolipid leaves the membrane, indicating that enhancement is not due to "vacancy defects". Mills and Needham hypothesize that the enhancement in permeability is due to lysolipid-stabilized pores in the micrograin boundary regions of the partially melted gel phase. However, the data only suggest the presence of pores, and the results do not provide firm evidence of their existence. One revealing experiment consisted of measuring the permeability of DPPC liposomes with incorporated monopalmitoyl-glycerol (GMP), a molecule identical to MPPC except with a less bulky headgroup. They saw no enhancement of dithionite permeability through DPPC−GMP liposomes as compared to pure DPPC liposomes. The difference is attributed to the difference in shape between GMP and MPPC, the former being more cylindrical and the latter being more conical. The conical shape of MPPC is thought to allow it to stabilize porous structures due to its ability to form a highly curved, hemispherical shape. As we will discuss later, our model does not pick up on this shape distinction; however our simulations do show the key role of the phase transition, a point that was clearly demonstrated in the experiments. In addition to DPPC, Mills and Needham examined liposomes comprised of palmitoyloleoylphosphatidylcholine (POPC) and MPPC by putting them through the same heating cycle as the DPPC−MPPC liposomes. They find only a small increase in permeability for the POPC−MPPC liposomes as POPC does not go through a phase transition and stays in

* To whom correspondence should be addressed: E-mail: schatz@chem.northwestern.edu.

10.1021/jp911309s
Published on Web 03/31/2010

the LC state throughout the experiment. This points to the importance of the gel to LC phase transition with regards the role of MPPC in enhancing permeability.

The permeation of water across lipid membranes has been simulated using atomistic molecular dynamics in studies by Marrink and Berendsen.[10] Permeation rates were deduced indirectly from the free energy and diffusion rate profiles across the bilayer. They found that both of these properties depend strongly on position in the membrane. The diffusion rate is highest in the middle of the membrane where the lipid density is lowest and the rate-limiting step is permeation through the dense part of the lipid tails where the resistance is greatest. Marrink and Berendsen calculated a water permeability coefficient through DPPC bilayers of $7(\pm 3) \times 10^{-2}$ cm/s, comparable to experimental values[11−13] if corrected for temperature. In a subsequent work, Marrink and Berendsen performed another set of similar simulations investigating the effects of size, hydrophobicity, and asphericity of the molecules on the permeation rate across lipid bilayers. They describe the bilayer with a four-region model. The regions include the low- and high-density headgroup regions, as well as the high- and low-density lipid tail regions, in that order, going from the edge of the bilayer to the center. Moderately hydrophilic and hydrophilic molecules (such as water) encounter the largest resistance to permeation in region 3, the dense part of the lipid tail region. Marrink and Berendsen also did an extensive study of the free volume properties of DPPC bilayers in which they found region 3 to closely resemble a soft polymer membrane.[14] With the development of a coarse-grained lipid model, Marrink et al.[15] were able to directly calculate a permeability coefficient for water crossing a DPPC lipid bilayer. They calculated a permeability coefficient of $1.5(\pm 0.5) \times 10^{-3}$ cm/s, the same order of magnitude as the experimentally measured permeability coefficients for pure DPPC vesicles.[12,13]

In a companion study to this work,[16] we utilized coarse-grained molecular dynamics (CGMD) to simulate DPPC−MPPC liposomes and examined their permeability to small solutes. Our goal was to compare the calculated permeabilities to experimental studies (also presented in that paper) of the release of the anticancer drug arsenic trioxide, As_2O_3,[17] from DPPC−MPPC liposomes. The CGMD simulations of liposomes were not able to assess the impact of the phase transition on the permeability as the coarse-grained model does not allow the formation of the gel phase in the liposome due to the high curvature. Hence, we are motivated in this study to simulate flat lipid bilayers which do form a gel phase upon cooling. In the liposome simulations, we observed permeability coefficients for water on the order of 1×10^{-3} cm/s, in good agreement with experiments[12,13] and previous CGMD simulations.[15] Above T_m, only a slight enhancement in permeability was observed upon addition of MPPC to the DPPC liposomes; similar results for the flat lipid bilayers will be demonstrated here. From the calculated permeability coefficients across the liposome bilayer we were able to estimate a half-time for liposome cargo release of 1 ms for a 100 nm diameter liposome. Phospholipids in the LC state are remarkably permeable to water, while the permeability of other uncharged polar solutes is generally at least 2 orders of magnitude smaller. Indeed, a molecule of more comparable size to arsenic trioxide is glycerol, for which the experimental permeability across phospholipids is measured to be 5×10^{-6} cm/s.[18] This value of P gives a halftime of release of 231 ms for a 100 nm diameter liposome. The conclusion of the liposome study was therefore that the release of As_2O_3 (which crosses the membrane as $As(OH)_3$) is likely to be slow, on the order of seconds. In the experimental results, the release of arsenic was determined to be slower than this, on the order of minutes, likely due to the rate-limiting step of redissolving the arsenic before it can cross the liposome membrane.

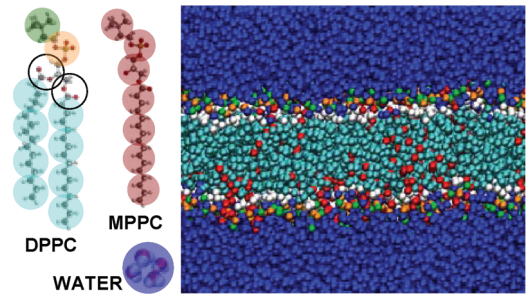

Figure 1. Coarse-grained representations of DPPC, MPPC, and water mapped onto the atomistic structures. The picture on the right is an example DPPC−MPPC bilayer surrounded by water at 325 K. There are 512 total lipids, 20% of which are MPPC. The hydration level is 16 coarse-grained waters/lipid (64 real waters/lipid). The DPPC choline group is in green, the phosphate group in orange, the glycerol group in white, and carbon tail beads in cyan. Waters are shown in blue and the MPPC lysolipids are shown in red. The bilayer image was created in Visual Molecular Dynamics.[31]

In this paper, we have used CGMD to model the permeation properties of flat DPPC bilayers with various amounts of incorporated MPPC lysolipid. CGMD is a recently developed simulation tool[15] that significantly reduces the computational size of a system, allowing the simulation of larger systems (such as biological systems) and longer time scales. The MARTINI coarse-grained force field,[19] which we use in this work, does form a stable gel phase upon cooling for DPPC bilayers. The only caveat is that the simulations form the untilted gel phase whereas experimentally a tilted gel phase is formed.[5] We assume that the impact of this difference on the permeability results is small. In the simulations, once the bilayer is cooled and the gel phase is formed, the system is heated back to the LC state to study the impact of the phase transformation on permeability. In addition to calculating the permeability coefficient for water crossing the bilayer membrane, we explore the mechanism for the enhancement of permeability upon inclusion of lysolipid.

II. Methods

A. System and Force Field. For the CGMD simulations we use the MARTINI force field developed by Marrink et al.[19] Details of the force field are given elsewhere[19] but we give a brief summary here. DPPC and MPPC are represented by 12 and 7 coarse-grained atoms, respectively. The coarse-grained atoms interact in a pairwise manner via a Lennard-Jones (LJ) potential. The mapping of real atoms onto coarse-grained atoms is done in a 4:1 ratio with approximately four nonhydrogen atoms forming one bead. For example, four methylene groups form one lipid tail bead. The lipid bilayer system consisted of 512 DPPC lipids and 8000 coarse-grained waters (16 CG waters/lipid). A small percentage (10%) of the CG waters were antifreeze waters (with a slightly larger radius) to keep the water from freezing as we lowered the temperature. To model DPPC/MPPC mixtures, we convert 5, 10, 15, 20, 30, 40, or 50% of the DPPC molecules in a bilayer to MPPC to create systems of varying concentrations. A snapshot of a DPPC bilayer with 20% MPPC is given in Figure 1 along with the coarse-grained representations mapped onto the atomic structures. Electron density profiles of the DPPC−MPPC(0%), DPPC−MPPC(20%), and DPPC−MPPC(50%) systems are shown in Figure 2. The electron density is calculated by weighting the bead density

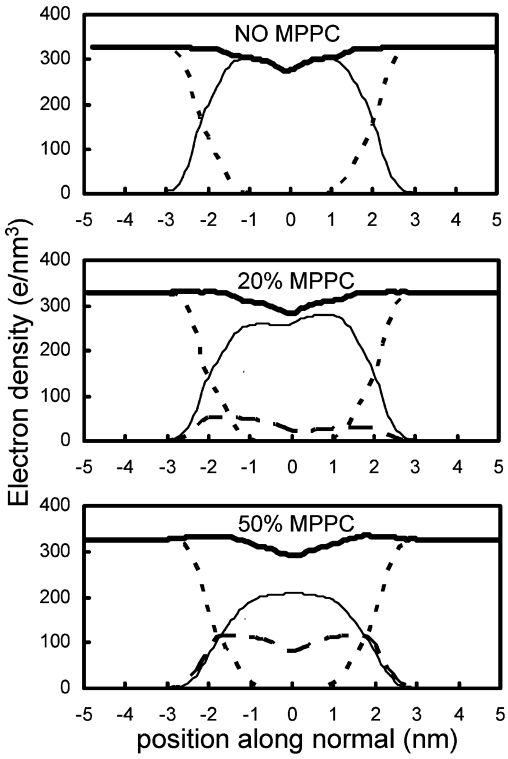

Figure 2. The top, middle, and bottom panels show the density profiles for pure DPPC, DPPC−MPPC(20%), and DPPC−MPPC(50%) bilayer systems, respectively. The center of the bilayer is located at 0 nm. The thin black, dotted, and dashed lines correspond to the electron density of the DPPC, water, and MPPC, respectively. The thick black line denotes the total electron density.

according to the number of electrons associated with each bead. The total electron density is similar for each system, however the DPPC electron density is decreased in the DPPC−MPPC(20%) and DPPC−MPPC(50%) systems due to the replacement of some DPPC by MPPC. In the bottom panel of Figure 2, note that even though there are equal numbers of DPPC and MPPC, the electron density of DPPC near the center of the bilayer is approximately twice that of the electron density of MPPC due to the double tail of DPPC. As can be seen from the electron density profiles, the MPPC lipids are evenly distributed throughout the bilayer.

B. Simulations Details. All simulations were carried out with the GROMACS molecular dynamics simulation software.[20] Three dimensional cubic periodic boundary conditions were used. The simulated system was kept at a constant pressure of 1 bar and a constant specified temperature (isobaric−isothermal NPT ensemble) using a Berendsen barostat and thermostat.[21] Semiisotropic pressure coupling was used. The systems were simulated for 1 μs with a time step of 40 fs. Coordinates were saved every 200 ps for analysis. Temperatures were chosen in 5 K increments between 285 and 325 K, below and above the gel to LC phase transition temperature of pure coarse-grained DPPC bilayers at 295 K.[22] Note that in the coarse-grained model there is a hysteresis in the phase-transition temperature depending on if the bilayer is being heated or cooled. The previously estimated phase transition temperature of 295 K for the coarse-grained DPPC bilayer[22] is based on the temperature where a half gel, half LC bilayer is stable. In the same study, it was noted that the apparent transition temperature upon cooling is near 285K, and upon heating is near 310K. In the present study we are not interested in absolute melting temperatures, and it is not viable for the DPPC/MPPC mixtures to perform calculations based on half gel, half LC mixtures, so we have chosen to restrict our melting temperature analysis to what we get from heating simulations.

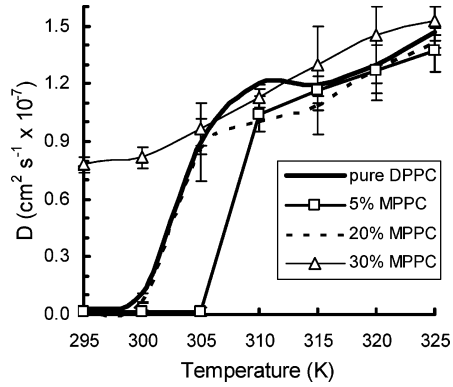

Figure 3. The diffusion constant of DPPC in four different bilayer systems is plotted as a function of temperature. The four systems include pure DPPC, DPPC−MPPC(5%), DPPC−MPPC(20%), and DPPC−MPPC(30%). The 10, 15, 40, and 50% MPPC systems are not shown for clarity. See text for details.

The dynamics of the CGMD simulations are significantly faster due to the smoother potential functions as compared with the fully atomistic potentials. This allows faster sampling of configuration space, however one must be careful with the interpretation of time in a CGMD simulation. The time scale presented in the results is an effective time scale. Since the diffusion rate of water in the CGMD simulation is four times faster than that of real water, the effective time scale can be interpreted as the actual time scale of the simulation multiplied by four.

III. Results and Discussion

A. Gel to Liquid-Crystalline Phase Transformation. The phase transition can be monitored by the area per lipid, the lateral diffusion coefficient, or the radial distribution function (RDF) of the lipids as the temperature is changed. We were unsuccessful in reproducing the "phase" of individual lipids as was done by Marrink et al. by determining lipid coordination numbers.[22] According to their analysis, a lipid molecule was considered to be in the gel phase if it had exactly six neighbors and that at least five of these neighbors were within a cutoff distance of 0.75 nm. As was done in ref 22, we calculated the number of nearest neighbors from a Voronoi analysis utilizing the Triangle program.[23] According to our Voronoi analysis, the distributions of the number of nearest neighbors surrounding each lipid were almost identical for the LC and gel phases. The distributions were indeed centered around six neighbors, however a distinction between the LC and gel phases could not be made on this basis. We were, however, able to verify the formation of the gel phase based on the decrease in the lipid lateral diffusion constant by 2 orders of magnitude, the decrease in area per lipid from 0.64 to 0.46 nm^2, as well as the change in RDF shape. From these properties, we were able to pinpoint the phase transition temperature to within $\pm$2 K. The experimental phase transition temperature, T_m, of pure DPPC bilayers transforming from gel to LC is near 315 K in reasonable agreement with our results as discussed below.

Figure 3 shows the lateral diffusion coefficient, D, of DPPC for various MPPC concentrations plotted as a function of temperature. In systems with $\leq$20% MPPC, we can see by the small value of D, 1.1($\pm$0.1) $\times$ 10^{-9} cm^2 s^{-1}, that the gel phase remains stable until the bilayer is heated to 300 K. For the pure

DPPC system, the LC phase begins to form near 300 K as shown by the sharp increase in D. The transition to the LC phase is complete by 315 K as D reaches $1.21(\pm 0.01) \times 10^{-7}$ cm^2 s^{-1}, 2 orders of magnitude larger than in the gel phase. Our simulation values of D are in good agreement with experiment[24,25] and previous simulations.[15] Upon converting 5% of the lipids to MPPC, the onset of the phase transition occurs near 305 K, 5 K higher than for the pure DPPC system, as can be seen in Figure 3. Although we omit the curves in Figure 3, the change in D with temperature for the DPPC−MPPC(10%) and DPPC−MPPC(15%) bilayers is essentially identical to that for the DPPC−MPPC(5%) bilayer. However, once a concentration of 20% MPPC is reached, the phase transition moves back to lower temperatures, with the plot of D versus temperature following the pure DPPC curve almost exactly. Examining both the RDF curves and the lateral diffusion coefficients as the bilayer is heated, we can estimate the phase transition temperature for each system. For the pure DPPC bilayer, we estimate the phase transition temperature (upon heating) to be 303 ± 2 K. The DPPC−MPPC(20%) bilayer undergoes the phase transition near this same temperature. The DPPC−MPPC(5%), DPPC−MPPC(10%), and DPPC−MPPC(15%) systems undergo the phase transition at a slightly higher temperature of 308 ± 2 K. This contrasts experimental measurements made by differential scanning calorimetry that shows that the addition of 10 mol % of MPPC to DPPC liposomes actually decreases the phase transition temperature between 1 and 2 K.[9] This difference appears to be an artifact of the coarse-grained model. It seems that adding small amounts of MPPC to the DPPC bilayer has a stabilizing effect on the gel phase, perhaps due to the shrinking of the area per lipid due to the presence of MPPC, similar to the way cholesterol elicits tighter packing in lipid membranes.[26] However, once the MPPC concentration reaches a certain threshold, in our case >20 mol %, the MPPC disrupts the packing of the DPPC enough to lower the phase transition temperature significantly. Thus the DPPC−MPPC(30%) bilayer did not form a gel phase for even the lowest-temperature simulations at 285 K, although the value of D at 285 K does drop to half its value at 325 K, indicating a mild drop in lipid mobility.

The RDF of the lipids also gives insight into the nature of the phase transition. Figure 4 plots the RDF between DPPC molecules in the gel and LC phases at temperatures below and above the phase transition temperature, respectively. The DPPC−MPPC(10%) and DPPC−MPPC(40%) MPPC systems are shown in the top and bottom panels of Figure 4, respectively. Note that only one curve is shown for the DPPC−MPPC(40%) systems because a gel phase does not form. However, for the DPPC−MPPC(10%) bilayer, there is a clear transition from the DPPC−DPPC RDF for the gel phase to the DPPC−DPPC RDF for the LC phase. In the gel phase, the DPPC−DPPC RDF is taller and sharper with fine structure indicating the ordering of the lipids. The DPPC−DPPC RDF in the LC phase is shorter and broader due to the more disordered nature of the LC phase and does not seem to depend on MPPC concentration. Figure 5 plots the RDF between DPPC and MPPC molecules at temperatures below and above the phase transition temperature. As with the DPPC results, the DPPC−MPPC RDF stays constant at all temperatures for systems with >20% MPPC. The distribution is relatively short and broad indicative of the LC phase. For systems with ≤20% MPPC, the DPPC−MPPC RDF below the phase transition is again sharp and narrow with some fine structure indicating some short-range order. Once the bilayer is heated above the phase transition temperature, the DPPC−MPPC

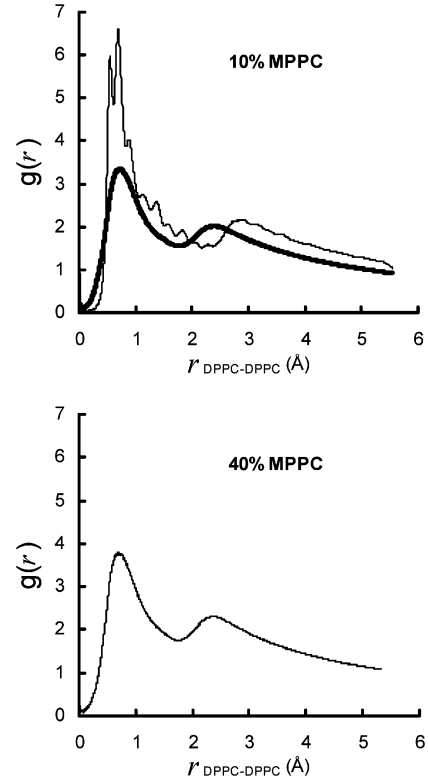

Figure 4. The DPPC−DPPC radial distribution function (RDF) for the DPPC−MPPC(10%) and DPPC−MPPC(40%) lipid bilayer systems. In the top panel, the thin and thick black lines show the RDFs when the bilayer is in the gel phase and liquid-crystalline phase, respectively. In the bottom panel, the RDF stays constant at all temperatures studied since no phase transition to a gel state was observed for systems containing 30% or more MPPC.

RDF broadens and loses the fine structure. Lastly, the MPPC−MPPC RDF is plotted in Figure 6. The gel phase curve for 10% MPPC exhibits a very tall and narrow peak and a clear periodicity to the fine structure in the tail of the curve. Once the bilayer converts to the LC phase, this fine structure is lost and the MPPC−MPPC RDF exhibits a shorter, broader peak, although not as broad as the corresponding DPPC−DPPC RDF or DPPC−MPPC RDF peaks. It makes sense that it would be narrower as at a concentration of only 10% MPPC, the most likely nearest neighor is a DPPC molecule rather than another MPPC.

B. Bilayer Permeability. To measure the permeability of the DPPC−MPPC lipid bilayers, we use coarse-grained water as our probe molecule. Coarse-grained water represents 4 molecular waters; however, because the sampling time of the simulations is sped up by approximately a factor of 4, this compensates for the coarse-graining of the water such that values close to experimental water permeabilities are obtained, as discussed below. Over the course of the CGMD trajectory, we monitor the bidirectional flux of water across the membrane. We then calculate the permeability coefficient from the following equation derived from Fick's law,[27] $P = J/\Delta CA$, where P is the permeability coefficient in cm/s, J is the unidirectional flux in mol s^{-1}, ΔC is the effective water concentration (55.5 mol dm^{-3}), and A is the surface area. The value of J is taken to be the average of the water flux in each direction through the bilayer (over long enough time periods these numbers should be equal).

Figure 7 plots the permeability coefficient P as a function of MPPC concentration for various temperatures. For MPPC concentrations between 0 and 20%, the membrane is very

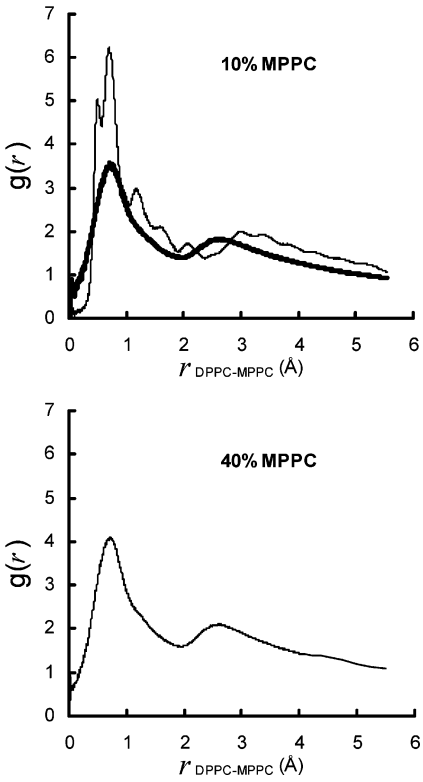

Figure 5. The DPPC−MPPC radial distribution function (RDF) for the DPPC−MPPC(10%) and DPPC−MPPC(40%) lipid bilayer systems. In the top panel, the thin and thick black lines show the RDFs when the bilayer is in the gel phase and liquid-crystalline phase, respectively. In the bottom panel, the RDF stays constant at all temperatures studied since no phase transition to a gel state was observed for systems containing 30% or more MPPC.

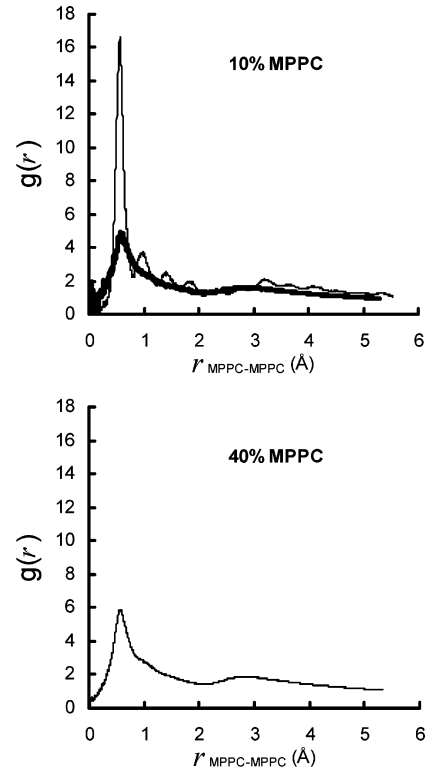

Figure 6. The MPPC−MPPC radial distribution function (RDF) for the DPPC−MPPC(10%) and DPPC−MPPC(40%) lipid bilayer systems. In the top panel, the thin and thick black lines show the RDFs when the bilayer is in the gel phase and liquid-crystalline phase, respectively. In the bottom panel, the RDF stays constant at all temperatures studied since no phase transition to a gel state was observed for systems containing 30% or more MPPC.

impermeable to water below 300 K since the bilayer is in the densely packed gel state. Generally, the more ordered and tightly packed the membrane, the less permeable it is.[28] For MPPC concentrations of 30−50%, a gel phase is never formed in our simulations so some permeability is observed for temperatures as low as 285 K. Once the bilayer reaches 315 K (above T_m for our coarse-grained model), permeability is observed at all MPPC concentrations with the permeability increasing slightly as the amount of MPPC increases. Upon further heating, the permeability of all the systems increases slightly at 320 K and increases significantly at 325 K. Between 315−320 K, the value of P is close to 1×10^{-3} cm/s whereas it doubles to approximately 2×10^{-3} cm/s at 325 K. These values are in good agreement with experimentally measured permeability coefficients of pure DPPC bilayers[11] as well as DPPC liposomes.[12,13]

The area per lipid as a function of MPPC concentration is plotted in Figure 8. As the amount of MPPC increases from 0 to 20% the area per lipid decreases from 0.47 to 0.42 nm^2 at 285 K when the bilayer is in the gel phase. These numbers are in good agreement with the experimentally determined area per lipid of 0.46 nm^2 for pure DPPC in the gel phase.[6] At 285 K, the area per lipid values for 30−50% MPPC are obviously higher as the gel phase is never fully formed, however the area per lipid still decreases with increasing MPPC−DPPC ratio. At 305 K, the system is very close to the phase transition and the area per lipid jumps up to above 0.60 nm^2. As the bilayer is further heated to 310 K, the area per lipid decreases slightly to values near 0.52−0.61 nm^2 with the values decreasing as the MPPC−DPPC ratio increases. When the bilayer is heated

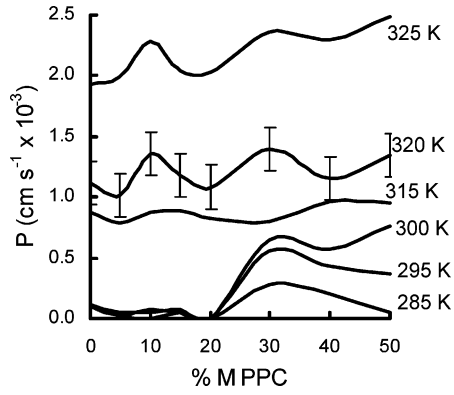

Figure 7. The water permeability coefficient P through the DPPC−MPPC bilayer as a function of MPPC concentration at various temperatures as labeled in the plot. The error bars are shown only on the 320 K curve for clarity.

to a final value of 325 K, the area per lipid again increases to values between 0.54−0.64 nm^2, in reasonable agreement with the experimentally determined value of 0.64 nm^2.[6]

Another representation of the permeability data is given in the top panel of Figure 9. Here we plot P as a function of temperature for several concentrations of MPPC. As mentioned above, for MPPC concentrations of 20% or less, very little permeability is seen at temperatures below T_m. In contrast, the permeability of the DPPC−MPPC(50%) bilayer never totally disappears, even at temperatures below the T_m for pure DPPC (similar behavior is seen for 30−40% MPPC). However, the lateral diffusion constant and area per lipid are decreased enough at these lower temperatures to still cause a significant lowering

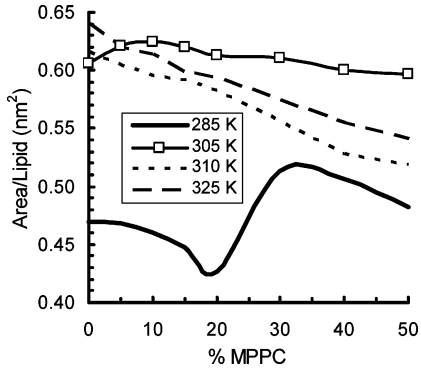

Figure 8. The area per lipid as a function of MPPC concentration for several temperatures as specified in the legend.

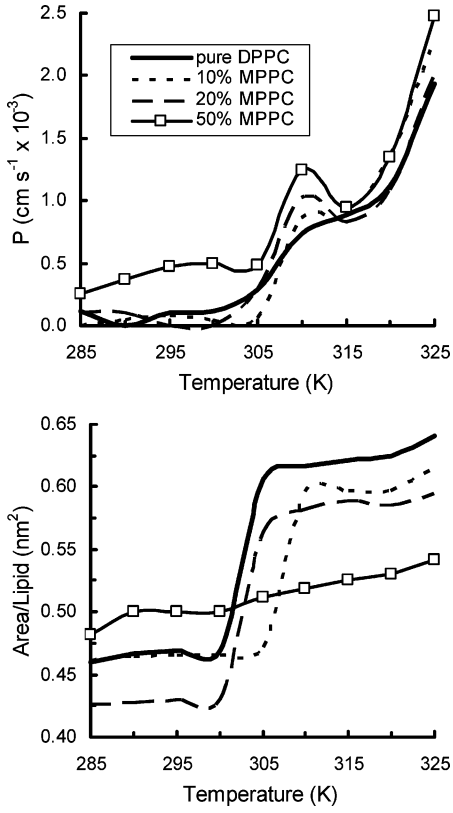

Figure 9. The top panel shows the water permeability coefficient P as a function of temperature for DPPC bilayers with varying concentrations of MPPC (0, 10, 20, and 50% MPPC). The results for 5, 15, 30, and 40% MPPC have similar profiles but are not shown for clarity. The bottom panel shows the area per lipid as a function of temperature for the same systems as in the top panel.

of the permeability even though a gel phase is not fully formed. As the bilayer is heated, the permeability shows very little change until the phase transition begins between 305 and 310 K. At the phase transition, the permeability of the bilayers increases dramatically and indeed peaks near T_m for those bilayers containing MPPC. This is the same behavior as seen in experiments.[9] The peak in permeability near the phase transition temperature correlates with a jump in the area per lipid as shown in the bottom panel of Figure 9. As the bilayer is heated, the area per lipid increases dramatically at the phase transition and continues to increase slowly as the bilayer is heated further to 325 K. Comparing the top and bottom panels of Figure 9 there is a clear correlation between the permeability and the magnitude of the area per lipid. Even though pure DPPC does go through a phase transition, we do not observe a definite

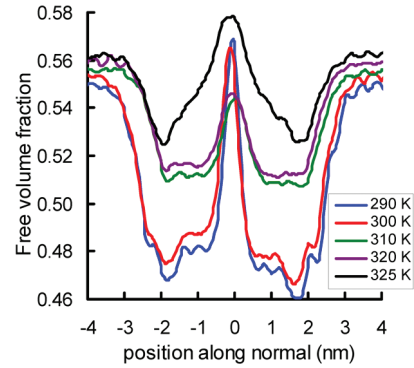

Figure 10. Free volume distribution of the DPPC−MPPC(20%) bilayer. Curves represent empty free volume along the direction normal to the bilayer as the bilayer is heated through the phase transition. The plot looks similar for other MPPC concentrations.

peak in the permeability near the phase transition temperature. However, the bilayers that contain the lysolipid do exhibit a well-defined peak near T_m.

Although the MPPC lysolipid is thought to stabilize pores in the bilayer of the DPPC liposome, we do not observe pores in our simulations. We must note that our model, though parametrized to represent the correct polarity of the MPPC headgroup, consists of coarse-grained beads of the same size so the effect of a conical shape is missing. In our simulations, the enhanced permeability upon addition of MPPC appears to be due to an increased free volume fraction in the bilayer caused by mismatches and a "missing tail" on the MPPC, as well as increased area per lipid near the phase transition and at temperatures >320 K. It has been shown in an atomistic molecular dynamics study by Bassolino-Klimas et al.[29] that the mechanism of diffusion of solutes through lipid bilayers occurs in part through jumps between voids, similar to that of small penetrants in soft polymers.[30] The size and frequency of the jumps vary with location in the bilayer. The jumps are larger and more frequent in the bilayer center where the tail density is lowest. Greater free volume in the bilayer would facilitate larger and more frequent jumps. Increased jump size and frequency directly correlate with higher diffusion coefficients and therefore higher permeability.

Figure 10 shows the free volume profile along the bilayer normal for the DPPC−MPPC(20%) system at several temperatures. The free volume is calculated by searching for vacuum space points in slabs 0.5 Å apart along the bilayer normal, using a grid point spacing of 0.5 Å in the plane of the bilayer. A point is considered in the vacuum if it lies outside the van der Waals radii of the water and lipid molecules. The overall shape of the free volume curves indicate that the largest free volume is found in the middle of the membrane. This correlates with the dip in total electron density at the center of the bilayer (see Figure 2). As the bilayer is heated from 290 to 300 K, the magnitude of free volume increases only slightly, whereas between 300 and 310 K, the bilayer undergoes the gel to LC phase transition and the free volume increases significantly. As the bilayer is heated to 320 K the free volume profile stays very similar to that at 310 K. By 325 K, the free volume increases again, correlating with the increase in permeability at this temperature as illustrated in Figure 9.

Finally, we examine the fluctuations in free volume in the LC phase for the different concentrations of MPPC. The free volume profiles for different MPPC concentrations at a single temperature varied only slightly. Instead, we calculated the standard deviation of the value of the free volume in each slab

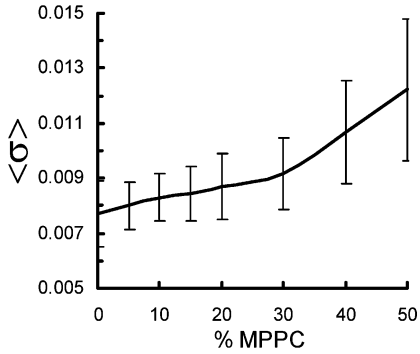

Figure 11. The values of the standard deviation in free volume fraction at 325 K when averaged along the normal to the bilayer from −2 to +2 nm as a function of MPPC concentration. The bilayer center is at 0 nm. At 325 K, all systems are in the liquid-crystalline phase.

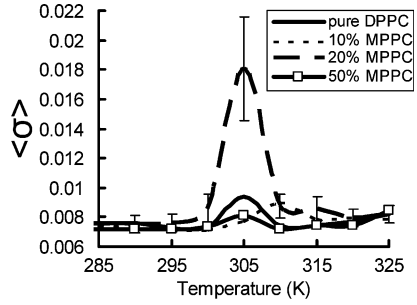

Figure 12. The values of the standard deviation in free volume fraction when averaged along the normal to the bilayer from −2 to +2 nm as a function of temperature. The bilayer center is at 0 nm. Each curve represents a different MPPC concentration as indicated in the legend.

and took the average of this number over the width of the bilayer, from −2 to 2 nm, along the coordinate normal to the bilayer with 0 nm being the center of the bilayer. This average standard deviation of the free volume fraction at 325 K is plotted in Figure 11 as a function of MPPC concentration. We see a mild increase in the average standard deviation of the free volume as the amount of MPPC increases. This suggests that more MPPC incorporated into the DPPC bilayer increases fluctuations in the free volume, leading to an increase in permeability. But as shown in Figure 7, in the LC phase the increase in permeability caused by MPPC is only on the order of 10−20% upon going from pure DPPC to DPPC−MPPC(50%). The increased fluctuations in free volume are partially compensated for by the shrinking of the area per lipid with increasing MPPC−DPPC ratio, so the increase in permeability with increasing MPPC concentration is modest. The results support the idea that the phase transition (coupled with inclusion of lysolipid) plays a significant role in the large enhancement of the permeability.

The effect of the phase transition on the fluctuations in free volume is shown in Figure 12. The magnitude of the fluctuations in free volume remains fairly constant as temperature is varied, except a peak is observed near the phase transition. The peak is largest for the 20% MPPC system, although as Figure 9 shows, the 20% system does not exhibit the largest peak in permeability. This lack of a direct correlation between fluctuations in free volume and permeability implies that large areas of free volume (i.e., pores) may not be the most important factor to permeability enhancement.

IV. Conclusions

In this work, we have used a coarse-grained model to investigate the enhanced permeability of lysolipid-incorporated lipid bilayers at the gel to LC phase transition. We found that indeed a peak in the permeability does coincide with the phase transition from the gel to LC state of DPPC bilayers when the lysolipid MPPC is present. This peak in permeability correlates with a sharp jump in the area per lipid near the same temperature as well as increased fluctuations in the lipid bilayer free volume. At temperatures above T_m, the permeability is only slightly dependent on the amount of lysolipid present. The increased free volume due to the "missing tail" of the lysolipid is partially compensated for by a decrease in area per lipid as the amount of lysolipid increases.

We were able to deduce the phase transition temperatures of the different DPPC−MPPC bilayer systems by monitoring the area per lipid, the lipid lateral diffusion constant, and the lipid−lipid RDF. In the coarse-grained model, a small amount ($\leq$15 mol %) of MPPC stabilizes the gel phase and increases the phase transition temperature by about 5 K, in contrast to experimental results where T_m is slightly lowered as compared to pure DPPC. Larger amounts of lysolipid destabilize the DPPC packing, leading to a reduction in the phase transition temperature. As a result, bilayers with 20 mol % MPPC had a phase transition temperature very near that of pure DPPC, and bilayers with $\geq$30% MPPC did not form a gel phase.

The enhanced permeability at the phase transition in our simulations appears to be due to a sharp jump in the area per lipid and increased fluctuations in the free volume near the phase transition temperature. No pores were observed in our simulations; however because our model does not accurately reflect the conical shape of the MPPC molecule, we cannot rule out the possibility of lysolipid-stabilized pores enhancing the permeability in the experiments.

Acknowledgment. The authors thank Siewert J. Marrink for helpful discussions and Wasut Pornpatcharapong for performing some of the calculations in this manuscript. This work was supported by the National Cancer Institute division of the U.S. National Institutes of Health as part of the Center of Cancer Nanotechnology Excellence at Northwestern University (U54CA119341).

References and Notes

(1) Yatvin, M.; Weinstein, J.; Dennis, W.; Blumenthal, R. *Science* **1978**, *202*, 1290–1293.
(2) Papahadjopoulos, D.; Jacobsen, K.; Nir, S.; Isac, T. *Biochim. Biophys. Acta* **1973**, *311*, 330–348.
(3) Demel, R. A.; Kruyff, B. D. *Biochim. Biophys. Acta* **1976**, *457*, 109–132.
(4) Chowdhry, B.; Lipka, G.; Dalziel, A.; Sturtevant, J. *Biophys. J.* **1984**, *45*, 901–904.
(5) Koynova, R.; Caffrey, M. *Biochim. Biophys. Acta* **1998**, *1376*, 91–145.
(6) Nagle, J. F.; Tristram-Nagle, S. *Biochim. Biophys. Acta* **2000**, *1469*, 159–195.
(7) Mouritsen, O.; Jorgensen, K.; Honger, T. Permeability of lipid bilayers near the phase transition. In *Permeability and Stability of Lipid Bilayers*; CRC Press: Boca Raton, 1995.
(8) Risbo, J.; Jørgensen, K.; Sperotto, M. M.; Mouritsen, O. G. *Biochim. Biophys. Acta* **1997**, *1329*, 85–96.
(9) Mills, J. K.; Needham, D. *Biochim. Biophys. Acta* **2005**, *1716*, 77–96.
(10) Marrink, S.; Berendsen, H. J. C. *J. Phys. Chem.* **1994**, *98*, 4155.
(11) Livne, A.; Graziani, Y. *J. Membr. Biol.* **1972**, *7*, 275–284.
(12) Carruthers, A.; Melchior, D. L. *Biochemistry* **1983**, *22*, 5797.
(13) Andrasko, J.; Forsen, S. *Biochem. Biophys. Res. Commun.* **1974**, *60*, 813.
(14) Marrink, S. J.; Sok, R. M.; Berendsen, H. J. C. *J. Chem. Phys.* **1996**, *104*, 9090–9099.
(15) Marrink, S. J.; de Vries, A. H.; Mark, A. E. *J. Phys. Chem. B* **2004**, *108*, 750–760.
(16) Winter, N. D.; Murphy, R. K.; Schatz, G. C.; O'Halloran, T. V. *J. Liposome Res.*, in press.

(17) Shen, Z.-X.; et al. *Blood* **1997**, *89*, 3354–3360.
(18) Lippe, C.; Gallucci, E.; Storelli, C. *Arch. Int. Physiol. Biochim.* **1971**, *79*, 315–318.
(19) Marrink, S. J.; Risselada, H. J.; Yefimov, S.; Tieleman, D. P.; de Vries, A. H. *J. Phys. Chem. B* **2007**, *111*, 7812–7824.
(20) Lindahl, E.; Hess, B.; Spoel, D. v. d. *J. Mol. Model.* **2001**, *7*, 306–317.
(21) Berendsen, H. J. C.; Postma, J. P. M.; van Gunsteren, W. F.; DiNola, A.; Haak, J. R. *J. Chem. Phys.* **1984**, *81*, 3684–3690.
(22) Marrink, S. J.; Risselada, J.; Mark, A. E. *Chem. Phys. Lipids* **2005**, *135*, 223–244.
(23) Shewchuk, J. R. *Comp. Geom.* **2002**, *22*, 21–74.
(24) Sheats, J. R.; McConnell, H. M. *Proc. Natl. Acad. Sci. U.S.A.* **1978**, *75*, 4661.
(25) Kuo, A. L.; Wade, C. G. *Biochemistry* **1979**, *18*, 2300.
(26) Smaby, J. M.; Brockman, H. L.; Brown, R. E. *Biochemistry* **2002**, *33*, 9135–9142.
(27) Cullis, P.; Fenske, D.; Hope, M. Physical properties and functional roles of lipids in membranes. In *Biochemistry of Lipids, Lipoproteins, and Membranes*, 3rd ed.; Vance, D., Vance, J., Eds.; Elsevier: New York, 1996.
(28) Gier, J. D.; Mandersloot, J.; Deenen, L. V. *Biochim. Biophys. Acta* **1968**, *150*, 666–675.
(29) Bassolino-Klimas, D.; Alper, H. E.; Stouch, T. R. *Biochemistry* **2002**, *32*, 12624–12637.
(30) Cohen, M. H.; Turnbull, D. *J. Chem. Phys.* **1959**, *31*, 1164–1169.
(31) Humphrey, W.; Dalke, A.; Schulten, K. *J. Mol. Graphics* **1996**, *14*, 33–38.

JP911309S